Surface volatilization modeling of (semi-)volatile hydrophobic organic compounds: The role of reference compounds

Douglas O. Pino-Herrera, Yannick Fayolle, Eric van Hullebusch, David Huguenot, Giovanni Esposito, Yoan Pechaud

Surface volatilization modeling of (semi-)volatile hydrophobic organic compounds: the role of reference compounds

Douglas O. Pino-Herrera [a,1,*], Yannick Fayolle [b], Eric D. van Hullebusch [c], David Huguenot [a], Giovanni Esposito [d], Yoan Pechaud [a*]

[a] Université Paris-Est, Laboratoire Géomatériaux et Environnement (EA 4508), UPEM, Marne-la-Vallée, 77454, France
[b] Université Paris-Saclay, INRAE, UR PROSE, 92160, Antony, France
[c] Institut de Physique du Globe de Paris, Sorbonne Paris Cité, Université Paris Diderot, UMR 7154, CNRS, F-75005 Paris, France
[d] University of Napoli "Federico II", Department of Civil, Architectural and Environmental Engineering, Via Claudio, 21, 80125 Napoli, Italy
*Corresponding authors: yoan.pechaud@u-pem.fr (Y. Pechaud), d.pinoherrera@brgm.fr (D. Pino-Herrera)

Abstract

Volatilization of hazardous hydrophobic organic compounds is often observed in many water, wastewater and soil treatment (bio)processes. Several models have been developed to quantify and predict gas-liquid pollutant transfer, being the proportionality coefficient model (PCM) one of the most commonly used, particularly in wastewater treatment. The PCM is based on the use of oxygen as a reference compound, which has a low resistance to the transfer in the gas phase. However, this resistance might be important for (semi-)volatile organic compounds – or (semi-)VOCs, which may render the use of the PCM model inaccurate. This study proposes an experimental methodology and a modeling approach for the use of the two-reference compound model (2RCM) that considers both the liquid-side and the gas-side resistances, by using water and oxygen as references. Results showed that the 2RCM predicts more accurately the overall mass transfer coefficients than the PCM for a VOC and two semi-VOCs tested in this study. In addition, the 2RCM was found to be a more robust method to estimate mass transfer coefficient of any compound and its use can be extrapolated to all substances. Finally, the relevance and limitations of both models was established.

Keywords

Volatilization; Mass transfer modeling; Mass transfer kinetics; Henry's law constant; HOCs; Reference compounds

[1] Current address: BRGM – Water, Environment, Process and Analyses Division, 3 Avenue Claude Guillemin – BP 36009 – 45060 – Orleans CEDEX 2, France

33 **Nomenclature**

34

A	Interfacial area for the mass transfer (m^2)
a	Interfacial area per unit of liquid volume ($m^2.m^{-3}$)
B	Constant in Eq. (22)
C_G	Concentration in the gas phase ($kg.m^{-3}$)
$C_{G,i}$	Concentration at the gas-liquid interface ($kg.m^{-3}$)
C_G^*	Equilibrium concentration in the gas phase ($kg.m^{-3}$)
C_L	Concentration in the liquid phase ($kg.m^{-3}$)
$C_{L,i}$	Concentration in the gas phase at the gas-liquid interface ($kg.m^{-3}$)
C_L^*	Equilibrium concentration in the liquid phase ($kg.m^{-3}$)
D	Reactor diameter (m)
D_G	Gas diffusivity ($m^2.s^{-1}$)
d_i	Impeller diameter (m)
D_L	Liquid diffusivity ($m^2.s^{-1}$)
DO	Dissolved oxygen ($mg.L^{-1}$)
H_C	Dimensionless Henry's law constant (-)
K_G	Overall mass transfer coefficient defined from the gas phase ($m.s^{-1}$)
k_G	Individual mass transfer coefficient in the gas film ($m.s^{-1}$)
$K_G a$	Overall volumetric mass transfer coefficient defined from the gas phase (s^{-1})
$k_G a$	Individual volumetric mass transfer coefficient in the gas film (s^{-1})
K_L	Overall mass transfer coefficient defined from the liquid phase ($m.s^{-1}$)
k_L	Individual mass transfer coefficient in the liquid film ($m.s^{-1}$)
$K_L a$	Overall volumetric mass transfer coefficient defined from the liquid phase (s^{-1})
$k_L a$	Individual volumetric mass transfer coefficient in the liquid film (s^{-1})
m	Gas diffusivity exponent (-)
N	Stirring speed (s^{-1})
$\dot{N}$	Mass transfer rate ($kg.s^{-1}$)
N_P	Power number (-)
n	Liquid diffusivity exponent (-)
p	Exponent in Eq. (22) (-)
$\frac{P_N}{V}$	Mechanical power input ($W.m^{-3}$)
Q_G	Airflow rate ($m^3.s^{-1}$)
r_c	Surface renewal rate (s^{-1})
R_G	Gas-side resistance to transfer ($s.m^{-1}$)
R_L	Liquid-side resistance to transfer ($s.m^{-1}$)
R_T	Total resistance to transfer ($s.m^{-1}$)
S_d	Saturation degree (-)
S_p	Slope (s^{-1})
t	time (s)
t_c	Contact time (s)

t_r	Bubble residence time (s)
V_G	Gas volume (m^3)
V_L	Liquid volume (m^3)

Greek letters

δ_G	Shear rate (s^{-1})
δ_L	Gas holdup (-)
Ψ	Proportionality coefficient (-)
ρ	Density ($kg.m^{-3}$)

Subscripts

G	Relative to the gas phase
HOC	Relative to Hydrophobic Organic Compound
i	Relative to the interface
L	Relative to the liquid phase
O_2	Relative to Oxygen
ref	Relative to a reference compound
W	Relative to Water

Superscripts

B	Relative to bubble volatilization
e	Estimated
in	Relative to the inlet
S	Relative to surface volatilization
out	Relative to the outlet

Acronyms

2RCM	Two-reference compound model
HOC	Hydrophobic organic compound
NAP	Naphthalene
PAH	Polycyclic aromatic hydrocarbons
PCM	Proportionality coefficient model
PHE	Phenanthrene
TOL	Toluene
VOC	Volatile organic compound

1. Introduction

Over the last decades, the occurrence of hazardous hydrophobic organic compounds (HOCs) as pollutants in the aquatic environments and soils has become a major environmental concern. Among the pollutants concerned, many are volatile and semi-volatile and can thus be transferred to the atmosphere due to mass transfer processes. Physicochemical and biological processes are often used to remove these pollutants during wastewater treatment, water purification treatments and soil remediation. In general, these processes need mixing to improve the homogeneity and the reactor performance and/or the introduction of a gas phase by a diffuser (aerobic biological treatment, ozonation, electro-Fenton, etc.) [1–5]. In systems open to the atmosphere, the mechanical power input promotes the surface aeration of the reactor, but it favors simultaneously the transfer of the most volatile molecules to the gas phase. In the same way, bubble dispersion through the liquid phase favors the transfer of the desired gas and at the same time the stripping of some volatile and semi-volatile compounds [6]. However, despite the environmental and public health issues, the volatilization process has been, in general, severely underestimated in wastewater treatment process [7] and even not considered in many research papers [5].

The most susceptible compounds to transfer are usually called volatile organic compounds (VOCs) and other compounds exhibiting the same behavior but in lesser extent (e.g. polycyclic aromatic compounds or PAHs) are frequently referred as “semi-volatile compounds”. In general, the Henry’s law constant determines the degree of volatilization of any compound [8]. However, the limit between the “volatile” and the “semi-volatile” categories is not clearly defined and there is no consensus in the literature regarding this issue. Furthermore, it is difficult to generalize because the extent of the volatilization does not only depend on the molecules properties but also on the local hydrodynamic conditions [9].

To predict the gas-liquid mass transfer rate of volatile and semi-volatile compounds, many authors have used oxygen as a reference molecule [10–12]. They relate the mass transfer coefficient of both the target compound and oxygen using a proportionality factor that only depends on the ratio of the diffusion coefficients of the two molecules. This approach assumes that the mass transfer is mainly controlled by the liquid-phase resistance, which tallies with the low solubility property of oxygen. Nevertheless, this is only valid for very volatile compounds. Conversely, for less volatile compounds for which the gas phase resistance cannot be neglected more complex models should be used [13].

In this sense, two models have been proposed to predict the mass transfer coefficient of (semi-)volatile molecules. The most complex is the two-reference compound model (2RCM).

To estimate the mass transfer coefficient of the molecule considered, the mass transfer coefficient of two reference molecules need to be known; one whose transfer is controlled by the gas phase and one whose transfer is controlled by the liquid phase [14]. The second model, called the proportionality coefficient model (PCM), uses the sum of resistances of one reference molecule (in general oxygen). Unlike the 2RCM, the PCM is based only on the measurement of the liquid-phase resistance. The gas phase resistance is then estimated. Only very few studies have been performed to validate these models and no comparison between them have been done [10,11,14,15]. In addition, most models require values of Henry's law constant (H_C) of the targeted compound. For many compounds, and particularly for HOCs, the range of values can be very wide, comprising several orders of magnitudes in some cases [16] which can lead to important errors in the estimation of the volatilization rates [17].

Therefore, there is a need to further investigate and to assess methodologies and models allowing predicting mass transfer of volatile and semi-volatile molecules. In this context, the objective of the present work was to study and model the gas-liquid surface mass transfer process of HOCs using both the PCM and the 2RCM. Three HOCs with different H_c values were selected as model molecules for the volatile and semi-volatile groups one VOC (toluene) and two PAHs (naphthalene and phenanthrene). The Henry's law constants of these compounds were experimentally estimated. Additionally, oxygen and water were used as the reference compounds. Experimental and modeling results were used to elaborate a comparative analysis of both the PCM and the 2RCM.

2. Mass transfer modeling

2.1. The two-film theory

According to the two-film theory, when a compound is transferred between two phases, it passes through two thin films that are formed on each side of the interface between these phases (Figure 1).

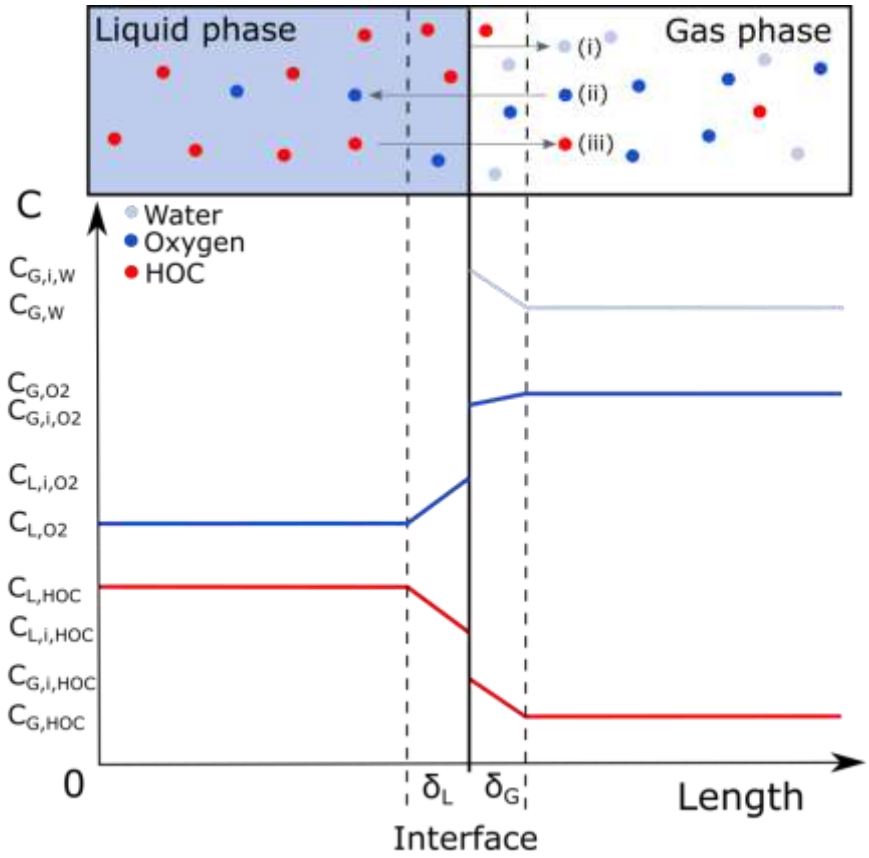

Figure 1. Two-film theory schema depicting three possible gas-liquid mass transfer processes: (i) evaporation, (ii) absorption and (iii) volatilization

The gradient of concentration in each layer decreases in the direction of the mass transfer and the relation between the concentrations at the interface is given by the Henry's law (Eq. (1)). Moreover, Henry's law defines also the equilibrium concentration of each phase through Eq. (2) and Eq. (3) [18–20].

$$C_{G,i} = H_c C_{L,i} \tag{1}$$

$$C_G^* = H_c C_L \tag{2}$$

$$C_L^* = \frac{C_G}{H_c} \tag{3}$$

Where $C_{G,i}$, C_G and C_G^* are respectively the gas interface concentration, the gas phase bulk concentration and the equilibrium concentration in the gas phase (kg.m^{-3}); $C_{L,i}$, C_L and C_L^* are respectively the liquid interface concentration, liquid phase bulk concentration and the equilibrium concentration in the liquid phase (kg.m^{-3}) and H_c is the dimensionless Henry's law constant (-).

Three possible cases are depicted in Figure 1: (i) the transfer of a liquid substance, such as water, to the gas phase at a temperature below its boiling point, known as evaporation; (ii) the transfer of a substance present in the gas phase, such as oxygen in air, into the liquid phase, called absorption; and (iii) the transfer of a substance dissolved in the liquid phase, in this case an HOCs, into the gas phase, usually called volatilization.

The mass transfer rate $\dot{N}$ for any compound moving from the liquid phase to the gas phase is given by Eq. (4) (in the liquid film) and Eq. (5) (in the gas film) [19,20].

$$\dot{N} = k_L A\left(C_L - C_{L,i}\right) \tag{4}$$

$$\dot{N} = k_G A\left(C_{G,i} - C_G\right) \tag{5}$$

Where k_L and k_G are the individual mass transfer coefficients respectively in the liquid film and in the gas film ($m.s^{-1}$) and A is the interfacial area (m^2).

If no accumulation in the layers is assumed, Eq. (4) and. Eq. (5) can be equalized. Then, invoking Henry's law (Eq. (1-3)), the transfer rate by unit of volume of a compound from the liquid phase to the gas phase can be calculated using either Eq. (6) or Eq. (7), depending on the phase in which the relation is applied [18].

$$\frac{dC_L}{dt} = K_L a(C_L^* - C_L) \tag{6}$$

$$\frac{dC_L}{dt} = K_G a(C_G - C_G^*) \tag{7}$$

Where $K_L a$ and $K_G a$ are the overall volumetric mass transfer coefficient defined respectively for the liquid phase and the gas phase (s^{-1}).

The $K_L a$ in Eq. (6) is equal to the inverse of the sum of the reciprocals of the mass transfer coefficient of both the liquid layer and the gas layer (corresponding to a sum of resistances), as shown in Eq. (8). This coefficient is related to the one defined for the gas phase (in Eq. (7)) by the Henry's law constant of the compound (Eq. (9)) [20].

$$K_L a = \frac{1}{\frac{1}{k_L a} + \frac{1}{H_C k_G a}} \;\; ; \;\; \frac{1}{R_T} = \frac{1}{R_L} + \frac{1}{R_G} \tag{8}$$

$$K_G a = H_C K_L a \tag{9}$$

Where R_T, R_L and R_G are respectively the total resistance to transfer, the liquid-side resistance to transfer and the gas-side resistance to transfer ($s.m^{-1}$).

For some compounds, the resistance in one of the phases can be considered negligible compared to the other phase. This is often the case for gases with low solubility (when the liquid phase is water), such as oxygen, that at standard conditions encounter very low resistance in the gas phase ($R_L \gg R_G$). Thus, $K_L a$ may be assimilated to the individual volumetric transfer coefficient of the liquid phase ($k_L a$) (Eq. (10)) and it is common to call these kind of processes "liquid-phase controlled mass transfer" [21].

$$K_L a \cong k_L a \tag{10}$$

Conversely, for the substances with a higher affinity for the liquid phase, the mass transfer can be considered "gas-phase controlled", meaning that the resistance in the liquid film can be considered negligible ($R_L \ll R_G$). In this case, $K_L a$ may be approximated to the individual volumetric transfer coefficient of the gas phase ($k_G a$) multiplied by the Henry's law constant (Eq. (11)).

$$K_L a \cong H_C k_G a \tag{11}$$

2.2. Mass transfer coefficient and diffusivity

Most models indicate that the mass transfer coefficient in each layer is proportional to the diffusivity raised to some power, as mentioned by Munz and Roberts [13] (Eq. (12) and Eq. (13)) .

$$k_L \propto (D_L)^n \tag{12}$$

$$k_G \propto (D_G)^m \tag{13}$$

Where D_L and D_G are the diffusivities respectively in the liquid and gas phase ($m^2.s^{-1}$) and n and m are respectively liquid and gas diffusivity exponents (-).

This means that, if the individual mass transfer coefficient in each layer of a reference compound and the exponent of the diffusivity term are known, it may be possible to estimate this parameter for any desired compound using Eq. (14) and Eq. (15).

$$\frac{k_L a}{k_L a_{ref}} = \left(\frac{D_L}{D_{L,ref}}\right)^n \tag{14}$$

$$\frac{k_G a}{k_G a_{ref}} = \left(\frac{D_G}{D_{G,ref}}\right)^m \tag{15}$$

Where $k_L a_{ref}$ and $k_G a_{ref}$ are respectively the $k_L a$ and $k_G a$ values of the reference compounds and $D_{L,ref}$ and $D_{G,ref}$ are respectively the D_L and D_G values of the reference compound.

Depending on the mass transfer theory used to relate the diffusivityand the mass transfer coefficient, as well as its underlying assumptions, *m* and *n* can take several values. Table 1 shows the expression of the relation in Eq. (14) for the main mass transfer theories existing in the literature. Analogously, the same relations can be applied for the gas film (Eq. (15)).

Table 1. Relation between the mass transfer coefficient and the diffusivity

Theory	Expression	Exponent n value	Reference
Two-film theory	$k_L = \frac{D_L}{\delta_L}$	1	[22]
Penetration theory	$k_L = 2\sqrt{\frac{D_L}{t_c}}$	0.5	[23]
Surface renewal theory	$k_L = \sqrt{D_L r_c}$	0.5	[24]

Where δ_L is the thickness of the liquid film (m), t_c is the contact time (s) and r_c is the surface renewal rate (s^{-1}).

In most studies, one of the theories and its corresponding value for m and/or n are chosen. However, some authors have estimated these values from experimental data by combining Eq. (8) and the ratio of diffusivities (Eq. (14) and/or Eq. (15)), which results in Eq. (16).

$$\frac{1}{K_L a} = \frac{1}{k_L a_{ref}\left(\frac{D_L}{D_{L,ref}}\right)^n} + \frac{1}{H_C k_G a_{ref}\left(\frac{D_G}{D_{G,ref}}\right)^m} \quad (16)$$

However, no consensus exists among the authors on the ranges, and even much less, on the specific values that these exponents might take [10,13,25,26].

Additionally, a number of empirical correlations exist that allow the calculation of the overall mass transfer coefficient for any substance in specific configurations [27,28]. However, it is important to observe the conditions in which the mentioned correlations are applicable.

3. Materials and methods

3.1. Experimental part

3.1.1. Reactor and operating conditions

The experiments were carried out in a standard 4.2-l glass reactor (working volume) with a thermal jacket controlled at 20 °C and four baffles. The dimensions of the reactor are specified by Pino-Herrera et al. [29]. Two reactor set-up configurations were used (Figure 2):

A) for Henry's law constant determination of HOCs, the gas phase was injected from the bottom of the reactor through a porous glass sparger connected to a three-port L-shaped valve, providing the choice between an air flow and a nitrogen flow as needed (Figure 2A); and B) for surface oxygen, water and HOCs mass transfer, the gas phase was introduced to the reactor using a plastic tube passing through holes in the lid, directing the air flow to the wall of the reactor. In this way, when the gas phase enters the reactor, preferential pathways for a direct exit and perturbations on the liquid surface were avoided (Figure 2B).

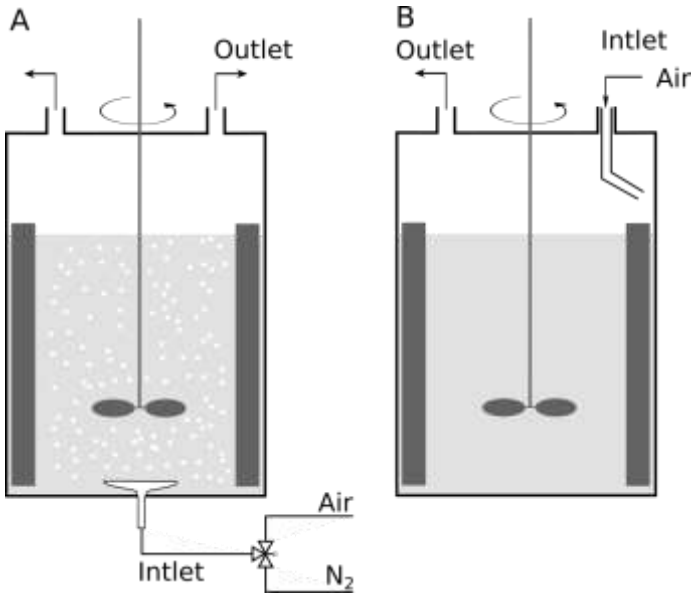

Figure 2. Experimental set-up: (A) Bubble mass transfer and (B) Surface mass transfer

Mechanical agitation was supplied by a motor with digital controlled stirring speed coupled with a single marine propeller ($d_i = D/3$, where D is the reactor diameter). The reactor was operated varying the corresponding operational parameters per test in the ranges given in Table 2. The power input was calculated using the power number (Eq. (17)). The power number N_P is constant and equal to 0.35 for a marine propeller at turbulent conditions ($Re > 10^4$), which is the case for all conditions tested in this study [30].

$$\frac{P_N}{V} = \frac{N_P \rho N^3 {d_i}^5}{V_L} \tag{17}$$

Where P_N/V is the mechanical power input (W.m^{-3}), N_P is the power number (-), ρ is the water density (kg.m^{-3}), N is the stirring speed (s^{-1}), d_i is the impeller diameter (m) and V_L is the liquid volume (m^3).

Table 2. Operational parameters used in this study.

Reactor configuration		Operational parameter	Units	Range
A	B			
	×	Q_G (×10^4) [a]	nm^3.s^{-1}	2.9
×		Q_G (×10^4) [b]	nm^3.s^{-1}	0.375 – 2.18
×	×	P_N/V	W.m^{-3}	17.65 – 94.52
×	×	T	°C	20

[a] surface airflow, [b] bubble airflow

3.1.2. HOC solutions and monitoring

3.1.2.1. HOC solutions

The HOCs used in this research work (toluene, naphthalene and phenanthrene) were obtained from Sigma-Aldrich chemicals (≥ 98% purity). Solvents (methanol and acetonitrile, HPLC grade) and phosphoric acid were obtained from VWR chemicals. Diffusivity of the compounds used in this study in air and water are shown in Table S1.

A solution of the three HOCs in water was prepared. For phenanthrene and naphthalene, a concentrated solution in methanol was previously prepared and 2 ml of this solution were added to 5 l of tap water, containing 3 ml of toluene. The amount of methanol in solution (< 0.04%) was low enough not to modify the mass transfer and the surface tension of the liquid in the system [31]. The solution was magnetically stirred until no droplets of toluene were observed and then filtered to remove any possible PAH crystals remaining in suspension before it was added to the reactor (4.2 L).

3.1.2.2. HOC concentration monitoring during mass transfer experiments

For each HOC mass transfer experiments, samples of the liquid phase were taken before and after starting either the bubble or the surface airflow at appropriate times and analyzed for HOC concentrations. Samples were measured using an HPLC (Hitachi *LaChrom Elite® L-2400)* coupled with UV/VIS detector (set to 254 nm) and a fluorescence detector (Excitation wavelength set to 250 nm and Emission wavelength set to 350 nm). The separation was performed using a RP C-18 end capped column (Purospher®, Merck) (5 mm, 25 cm × 4.6 mm) placed in an oven at 40 °C. The mobile phase was a mixture of water (at pH adjusted

to 2.5 using phosphoric acid) and acetonitrile (25:75 v/v) with a flow rate of 0.8 ml.min^{-1} in isocratic mode. The injection volume was 20 µl.

3.1.3. HOC Henry's law constant determination in bubbly reactor

The theoretical development for the determination of Henry's law constant is developed in Appendix A. For the Henry's law constant determination of the selected HOCs, the reactor set-up configuration shown in Figure 2A was used. An HOC solution was prepared as explained in section 3.1.2 and introduced in the reactor (4.2 l) and, after introducing the bubbly flow, the depletion of the HOC concentrations in the liquid phase was measured over time. Experiments were performed adjusting the operating parameters within the ranges given in Table 2.

3.1.4. Surface mass transfer in gas and liquid films

3.1.4.1. Oxygen mass transfer coefficient

The oxygen transfer coefficients were obtained using the configuration shown in Figure 2B and were measured using the dynamic method (gassing out), described by García-Ochoa and Gomez [21]. The curve of oxygen absorption was recorded using an inoLab® Oxi 7310 DO sensor connected to a Cellox 325 probe (WTW). From the oxygen absorption curves, the surface oxygen mass transfer coefficients ($k_L a_{O_2}^S$) in Eq. (18) were estimated, taking into account the response time of the electrode. The influence of power input on this parameter was measured within the range shown in Table 2.

$$\frac{dC_{L,O_2}}{dt} = k_L a_{O_2}^S \left(C_{L,O_2}^* - C_{L,O_2}\right) \tag{18}$$

Where subscript O_2 refers to oxygen, superscript S refers to surface.

3.1.4.2. Water mass transfer coefficient

The water transfer coefficients were obtained using the configuration shown in Figure 2B. An airflow was continuously introduced to the upper part of the experimental system and steady state conditions in the gas phase was reached. Then, the gas phase relative humidity and temperature was measured using a KIMO® AMI 310 multifunction meter at the inlet and the outlet of the reactor. The airflow was introduced in the gas phase from the top of the reactor, avoiding disturbances in the liquid surface and the saturation of the gas phase. The surface

water transfer coefficient was subsequently obtained by performing a mass balance for the humidity in the gas phase (Eq. (19)), knowing the psychrometric conditions of the air at the inlet and the outlet of the reactor.

$$C_{G,W}^{in} Q_G + k_G a_W^S \left(C_{G,W}^* - C_{G,W}\right) = C_{G,W}^{out} Q_G \quad (19)$$

Where $C_{G,W}$ is the vapor concentration in air, the superscripts in and out refer respectively to the inlet and outlet airflow, the subscript W refers to water and $C_{G,W}^*$ is the saturated vapor concentration calculated at the air temperature using the equilibrium vapor pressure correlation developed by Lowe [32]. Since $C_{G,W}$ varies throughout the reactor headspace, the logarithmic mean vapor concentration between the inlet and outlet airflow was used in order to estimate the driving force for water evaporation along the water surface.

Several airflow rates (Q_G) were tested for all agitation conditions to check that this parameter did not affect the transfer coefficient and that the saturated vapor concentration was not reached in the outlet airflow. An average airflow rate on the surface of 2.9×10^{-4} $m^3.s^{-1}$ was fixed. The influence of power input on this parameter was measured within the range shown in Table 2.

3.1.4.3. Surface HOCs mass transfer coefficient

The overall HOC surface mass transfer coefficients were obtained using the reactor set-up configuration in Figure 2B. An HOC solution was prepared as explained in section 3.1.2 and introduced in the reactor. An airflow was introduced from the top of the reactor through the lid avoiding disturbances in the liquid surface to remove any accumulation of HOCs in the gas phase. In this case, HOC gas phase concentration was considered negligible, since the gas phase was continuously renewed (concentration in the inlet gas $C_G = 0$). This hypothesis was further confirmed by demonstrating the nominal gas phase HOC concentration (maximal HOC mass flux divided by Q_G) was negligible in comparison with the $C_{G,HOC}^*$.

A batch volatilization experiment where the HOC concentration was measured as a function of time led to a first order equation from which the HOC surface mass transfer coefficient was easily calculated (Eq. (6)). The influence of power input on this parameter was measured within the range shown in Table 2.

3.2. HOC mass transfer modeling

In this study, two models to predict the individual and the overall gas-liquid mass transfer coefficients of the HOCs were tested and compared: the 2RCM and the PCM.

3.2.1. Two-reference-compound model (2RCM)

In liquid-controlled mass transfer processes, oxygen is often used as reference compound because its gas-side resistance can be considered negligible and Eq. (10) can be applied. Conversely, in aqueous solutions, water presents a virtually non-existent transfer resistance in the liquid phase, which allows the use of Eq. (11). Then, by introducing oxygen and water as reference compounds in Eq. (16), the HOC mass transfer coefficient could be estimated using Eq. (20).

$$\frac{1}{K_L a^S_{HOC}} = \frac{1}{k_L a^S_{O_2} \left(\frac{D_{L,HOC}}{D_{L,O_2}}\right)^n} + \frac{1}{H_C k_G a^S_W \left(\frac{D_{G,HOC}}{D_{G,W}}\right)^m} \quad (20)$$

The exponents of each diffusivity ratio (m and n) were chosen according to the hydrodynamic conditions expected at each side of the interface as explained in section 3.2.3. The HOC mass transfer coefficients estimated using the experimental oxygen and water mass transfer coefficients and the Henry's law constant for each HOC were compared to those obtained experimentally and the deviations were calculated for each compound tested.

3.2.2. Proportionality coefficient model (PCM)

Hsieh et al. [11] transformed Eq. (16) by using only oxygen as the reference compound and defining the proportionality coefficient (Ψ) as shown in Eq. (21). This relation was also tested by fixing both exponents n and m as described in section 3.2.3. However, in this case, the ratio of individual oxygen mass transfer coefficients ($k_G a^S_{O_2}/k_L a^S_{O_2}$) was not known. Thus, this parameter was estimated using the experimental Ψ obtained for each HOC tested in this study at different power input conditions.

$$\Psi = \frac{K_L a^S_{HOC}}{K_L a^S_{O_2}} = \frac{1}{\frac{1}{\left(\frac{D_{L,HOC}}{D_{L,O_2}}\right)^n} + \frac{1}{H_C\left(k_G a^S_{O_2}/k_L a^S_{O_2}\right)\left(\frac{D_{G,HOC}}{D_{G,O_2}}\right)^m}} \quad (21)$$

Figure 3 shows a scheme of the parameter estimation followed in this study. First, from the experimental data and an assumed $k_G a^S_{O_2}/k_L a^S_{O_2}$, the HOC overall mass transfer coefficients for each power input tested were calculated. Then, the sum of the squared errors between the

calculated coefficients and the experimental ones was minimized by modifying the initial assumed parameters. Once the minimal error was reached, the estimated and calculated parameters for each model were analyzed and compared. Both models were tested and compared based on their accuracy and their robustness to predict HOC overall mass transfer coefficients.

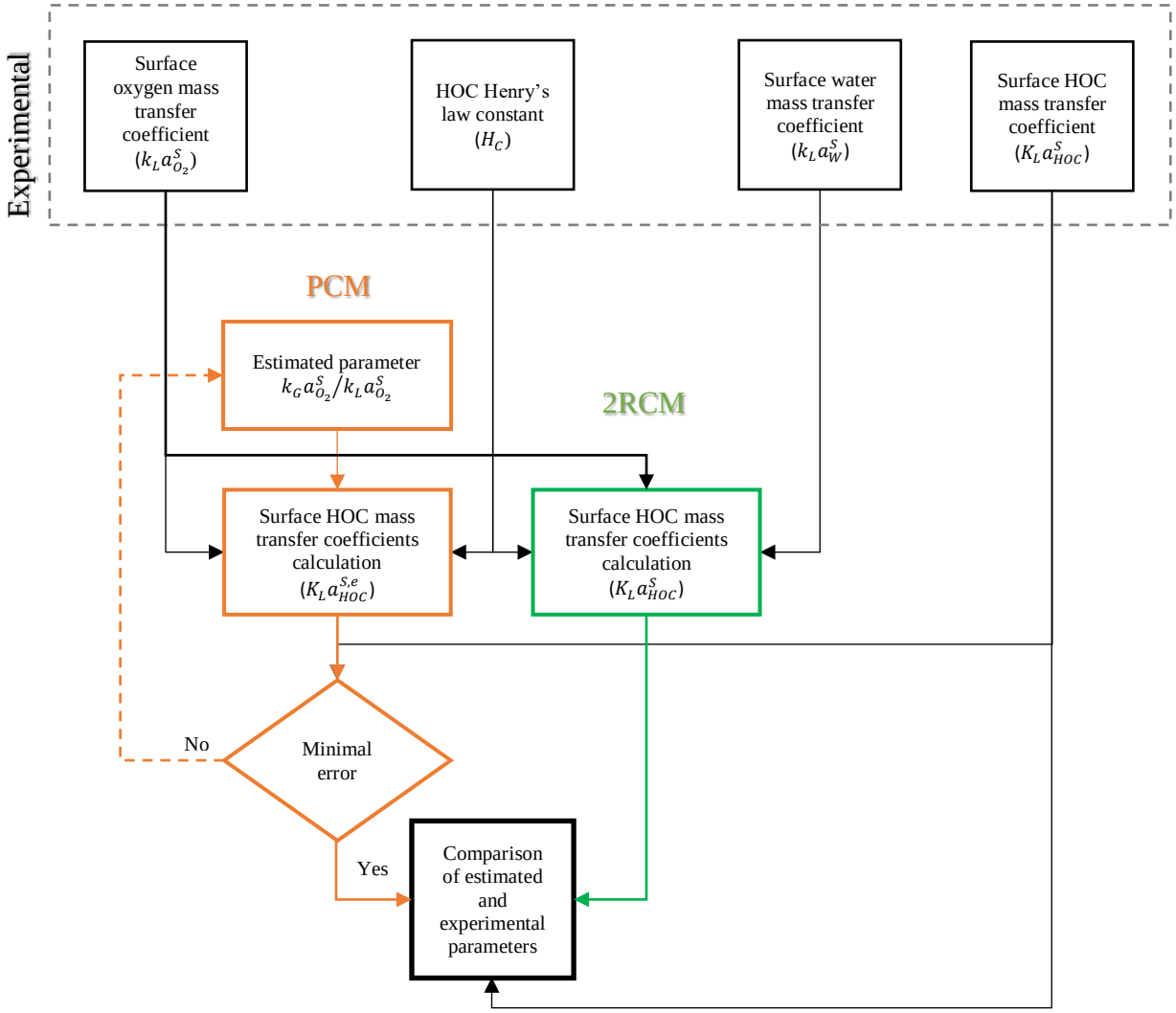

Figure 3. Modeling approach using the proportionality coefficient modem (PCM) and the two-reference-compound model (2RCM)

3.2.3. Selection of the diffusivity exponents (*n* and *m*)

In order to predict HOC mass transfer coefficients using Eq. (20) and Eq. (21), it is necessary to estimate or to fix the values for the exponents *m* and *n*. Several approaches for this estimation have been used in the literature, but, in general, they imply some assumptions that are difficult to test experimentally. For example, Hsieh et al. [11], Soltanali and Shams Hagani [26] and Munz and Roberts [13], assumed that both exponents are equal, due to the

uncertainty in their calculation and the lack of information regarding the parameters influencing them. Additionally, the latter authors have found that the diffusivity exponents are virtually independent of the mixing intensity. Moreover, some authors, such as Chrysikopoulos et al. [33], Smith et al. [14] and Libra [34], have considered that the diffusivity exponents depend on the type of compound. Since there is no consensus among the authors, the values for these exponents were fixed according to the hydrodynamic conditions at each side of the interface in this study. For the liquid side, the exponent n was fixed to 0.5, which correspond to Higbie's penetration theory that is typically applied for turbulent regimes [23]. In the case of the gas side, the mixing regime was not completely defined. Thus, the exponent m was fixed to a value of 1, corresponding to the two-film theory [24].

4. Results and discussion

4.1. HOC Henry's law constant

To calculate the Henry's law constant by the method described in section 3.1.3, the compound saturation concentration when the bubbles leave the liquid phase in the reactor need to be reached. Given that it was not possible to measure the gas phase concentration for the experiments performed in this study, indirect methods to ensure the bubble saturation were used. A linear relation was observed between the slope for bubble volatilization experiments tested (Sp^B) and the airflow rate at different mechanical power inputs (Figure S1). Likewise, there is no significant effect of the mechanical power input on this parameter. These corroborations allow to draw the conclusions that, for the three molecules tested in this research work, saturation was reached [17] and that the bubble residence time was negligible in comparison to the variation of C_L in time (Eq. (A.2)).

The results for the H_C calculation are reported in Table 3. The calculated values for the Henry's law constant are within the range of those found in the literature, which further confirms the hypothesis of the bubble saturation. Additionally, it is interesting to observe that the Henry's law constants for HOCs presented in Table 3 show a wide range of values. This might be due to the different experimental set-ups and conditions in which they have been measured. Therefore, as H_c is a key parameter, it should be obtained experimentally whenever possible.

Table 3. Estimated Henry's law constants and comparison with literature values.

Compound	H_C estimated (-)	Range of experimental H_C reference values*

Toluene	1.78×10^{-1}	$1.46\times10^{-1} – 5.26\times10^{-1}$
Naphthalene	1.44×10^{-2}	$6.84\times10^{-3} – 3.16\times10^{-2}$
Phenanthrene	1.04×10^{-3}	$9.77\times10^{-4} – 2.56\times10^{-3}$

*According to the H_C compilation made by Sander [16]

4.2. Surface mass transfer

4.2.1. Oxygen and water

Figure 4 shows the results of the test performed to measure the influence of P_N/V on the surface mass transfer coefficients of oxygen ($k_L a^S_{O2}$) and water ($k_G a^S_W$). These coefficients are positively correlated to P_N/V. In addition the trends in both cases follow a power-type curve fit, which is in accordance with the literature for many compounds [11,13,21]. However, for oxygen transfer, the power coefficient is five times higher than the one for water transfer.

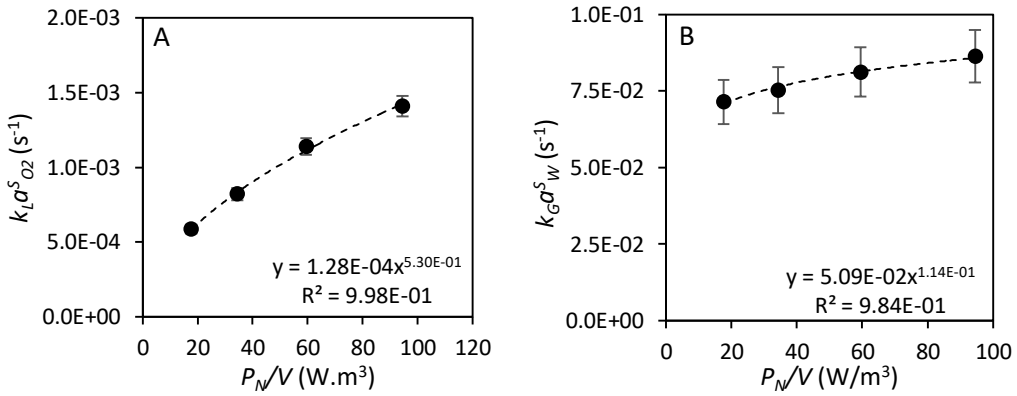

Figure 4. Influence of the power input on the surface mass transfer coefficient for (A) Oxygen and (B) Water.

The P_N/V increases can lead to two effects at the surface:(i) since the agitation is being directly applied to the liquid phase, it induces a faster surface renewal (or a decreased film thickness) at the liquid side of the surface; (ii) higher agitation produces an increase of the gas-liquid interfacial area due to surface deformation. This effect was visible to the naked eye in the reactor. Since oxygen is transferred from the gas phase to the liquid phase, both phenomena affect its transfer. However, the continuous liquid phase is constituted by water, which means that the water transfer occurs at gas side of the gas-liquid interface. Hence, the first effect does not have any consequence and only the gas-liquid interfacial area

modification is influencing this water transfer. These phenomena can explain the significant difference in the influence of the power input in the transfer of these two substances. Additionally, the exponent of the power relation for the oxygen transfer is in agreement with the results found by Hsieh et al. [11] for similar operating systems.

4.2.2. HOC

In the same way as for water and oxygen transfer, the surface volatilization coefficient of HOCs depends on the power input. The relation between $^{P_N}/_{V}$ and the mass transfer coefficient ($K_L a^S_{HOC}$) can be assimilated to a power model in the range of $^{P_N}/_{V}$ tested in this study (Figure 5).

$$K_L a^S_{HOC} = B\left(\frac{P_N}{V}\right)^p \tag{22}$$

Where B and p are empirical constant values.

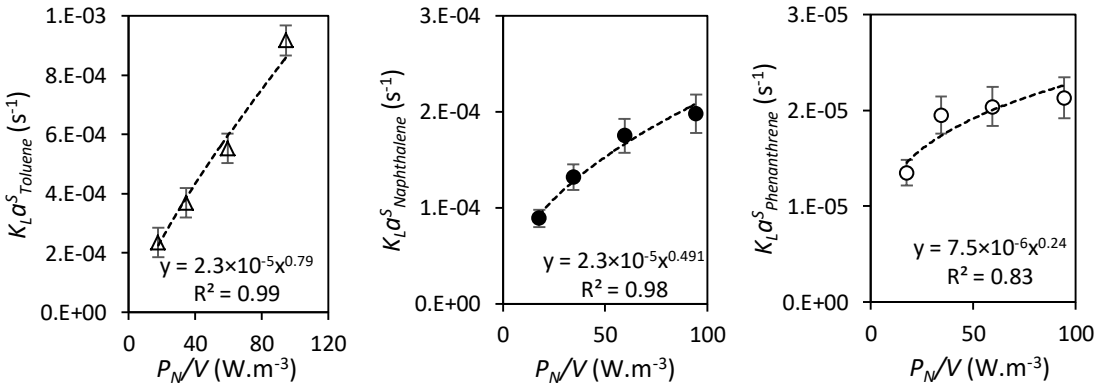

Figure 5. Influence of power input on the surface mass transfer coefficient for (▵) Toluene, (●) Naphthalene and (○) Phenanthrene

Moreover, a linear positive dependence of p and the natural logarithm of H_C of the HOCs can be established (Figure 6). This can be explained by the effect of $^{P_N}/_{V}$ on the mass transfer coefficient of the liquid side of the interface. In fact, $^{P_N}/_{V}$ has a direct impact on the liquid side and increases at a higher extent the overall mass transfer coefficient of the more volatile compounds. Thus, the volatilization of semi-volatile compounds is less affected by $^{P_N}/_{V}$, because the gas-side transfer resistance is comparable or higher than the liquid-side transfer

resistance ($R_G \approx R_L$). The correlation proposed in Figure 6 can be used to estimate the extent of the impact of the power input on the volatilization rate for HOCs.

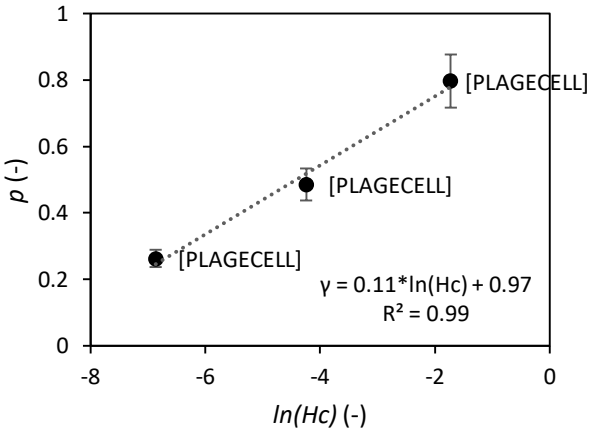

Figure 6. Correlation between p and ln(H_C).

It is interesting to notice that the p value is higher for toluene than for oxygen, which is probably due to changes in the surface properties of the toluene solution. However, further research is needed on the impact of the modification of surface properties on the film resistances and the mass transfer.

4.3. Modeling of surface HOC mass transfer coefficient

The two previously presented models (PCM and 2RCM) were tested employing the experimental data obtained for the surface transfer of HOCs, water and oxygen.

The PCM required the use of oxygen as the only reference compound makes possible to neglect the resistance in the gas phase for the reference compound (due to the high H_C value for oxygen). For this model, the ratio of individual volumetric mass transfer coefficients for the oxygen ($k_G a^S_{O_2}/k_L a^S_{O_2}$) is estimated. Since each individual mass transfer coefficient is influenced differently by the mixing in the reactor, their ratio changes with a variation of P_N/V. Therefore, the estimation was made assuming one $k_G a^S_{O_2}/k_L a^S_{O_2}$ for each considered P_N/V.

The 2RCM is a more general approach than the PCM for the volatilization modeling of semi-volatile substances [26]. To test the 2RCM, oxygen and water were used as reference compounds for the liquid-side and gas-side mass transfer resistance, respectively. No parameters need to be estimated using this model, since both individual mass transfer coefficient were calculated experimentally, and the diffusivity exponents were fixed.

Figure 7 shows the correlation between the experimental and the calculated values for the overall mass transfer coefficient of the three HOCs tested in this study for the PCM and the 2RCM. The PCM fits rather well to the most volatile compound (toluene), but much higher error values are obtained for the least volatile ones (naphthalene and phenanthrene). Moreover, the plot between the calculated and the experimental overall mass transfer coefficients presents a good correlation ($R^2 = 0.96$). On the other hand, the 2RCM model fits much better for naphthalene and phenanthrene, but the difference between the experimental and estimated $K_L a^S_{HOC}$ increase for toluene. Additionally, the goodness of fit is slightly better than that of the PCM ($R^2 = 0.978$) and most values are within the 30% error. This means that the 2RCM seems to predict better the overall mass transfer coefficient for the three substances tested. In addition this result shows that depending on the ${}^{P_N}/_{V}$ value and thus on the hydrodynamic conditions the error can vary.

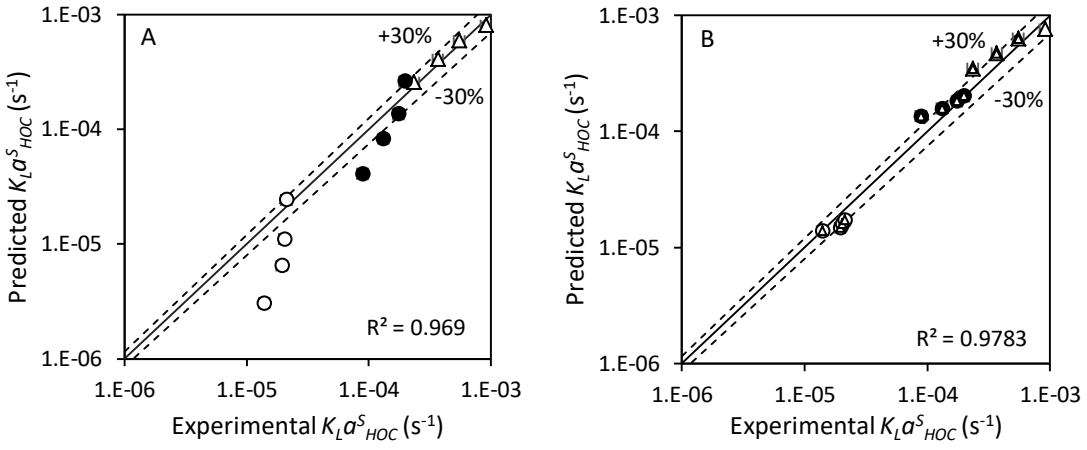

Figure 7. HOC mass transfer coefficients correlation for: (A) the PCM; and (B) the 2RCM; for (▵) Toluene, (●) Naphthalene and (○) Phenanthrene in logarithmic scale.

In terms of reference compounds, most authors have used the PCM model due to the convenience of utilizing oxygen as the only reference compound. Thus, very few studies have used other substances as reference compounds, much less for estimating the gas-side mass transfer coefficient. Monteith et al. [35] suggested the use of ammonia for this purpose due to its low Henry's law constant, but the ionization of this compound in water and the influence of pH on the mass transfer may complicate the experiments and the analytical processing of the data. In fact, high ion concentrations and changes in surface tension can modify the mass transfer coefficient of any compound [36]. In the present paper, we chose to use water as a reference compound for the surface mass transfer of semi-volatile compounds. This choice was based on the following advantages (Smith et al. [14]): i) its transfer has virtually no

458 resistance in liquid-phase film; ii) the measurement of water concentration in the gas phase is
459 relatively easy to perform; and iii) it is an economic and fast method to obtain information for
460 the gas-side mass transfer.
461 Besides, using Eq. (15) and taking water as a reference compound, it is possible to obtain the
462 gas-side oxygen mass transfer coefficient ($k_G a_{O_2}^S$) and, thus, to obtain the ratio of individual
463 oxygen mass transfer coefficients ($k_G a_{O_2}^S / k_L a_{O_2}^S$) by a simple calculation. The estimated
464 $k_G a_{O_2}^S / k_L a_{O_2}^S$ values for the PCM were then compared to the calculated ones using the 2RCM
465 model (Table 4). It is important to highlight that the values obtained by both methods are in
466 the same order of magnitude of those found by Munz and Roberts [13], but much lower than
467 those found by Hsieh et al. [11]. This can be explained by the different geometry and the
468 hydrodynamic properties of the reactor in both phases.
469 Moreover, the calculated ratio decreases as the mixing intensity augments. Considering that
470 the P_N/V was directly applied to the liquid phase and that the gas phase was fed with the same
471 Q_G throughout all the experiments, the obtained relation seems quite logical. In fact, when
472 P_N/V increases, the renewal rate at the liquid interface augments, increasing the individual
473 oxygen mass transfer coefficient in the liquid phase (k_L), while the flow properties in the gas-
474 side of the interface remains almost unchanged. This can be translated in less important k_G
475 variations in comparison with $k_L$variations, particularly for oxygen since its transfer is liquid-
476 phase controlled. Consequently, $k_G a_{O_2}^S / k_L a_{O_2}^S$ decreases when P_N/V increases.
477 However, for the ratio estimated using the PCM, the ratio increase with P_N/V. This trend
478 contradicts the results calculated using water as reference compound and it is a direct
479 consequence of using semi-volatile compounds for fitting the PCM using oxygen. Indeed,
480 small changes in the gas-phase film can highly influence the transfer of semi-volatile
481 compounds and this cannot be taken into accounted by the PCM with oxygen as the sole
482 reference compound, distorting the relation between power input and $k_G a_{O_2}^S / k_L a_{O_2}^S$.
483
484 *Table 4.* $k_G a_{O_2}^S / k_L a_{O_2}^S$ *ratio calculated using water as reference compound and estimated for the PCM and*
485 *calculated*

$\frac{P_N}{V}$ (W.m^{-3})	$k_G a_{O_2}^S / k_L a_{O_2}^S$ (-)	
	Estimated by the PCM	Calculated

17.65	15.8	74.1
34.37	24.1	55.9
59.47	29.7	43.4
94.52	53.5	37.3

In addition, with the purpose of testing the hypothesis made previously on the exponent values $n = 0.5$ and $m = 1$ and since the 2RCM does not requires the fitting of any parameter, an estimation of both n and m was done using this model with a minimization of the sum of the squared errors between the calculated and the experimental mass transfer coefficients. As a result, the best fitting for n and m was found for values of 0.53 and 1.01, respectively (R^2 = 0.98). This confirms the hypothesis behind the choice of these parameter values.

4.4. (Semi-)Volatile nature of HOCs

Many authors consider that the "volatile" characteristic of a dissolved compound in terms of mass transfer is mainly given by its Henry's law constant. Although there is no definitive consensus on the matter, in general, compounds with $H_C \geq 0.19$ are considered volatile and thus their mass transfer is considered to be liquid-phase controlled [37]. Besides, some authors consider that the liquid-side resistance is only completely negligible for compounds with $H_C \geq 0.55$ [26]. According to these definitions, toluene is placed around the limit of the "volatile" category (H_C = 0.178). Low-molecular-weight PAHs (i.e. naphthalene and phenanthrene) are generally considered "semi-volatile" compounds [14,38], presenting a much more important gas-phase resistance [39]. Nevertheless, some authors also consider naphthalene as a volatile compound [11,40]. This proves that the limit between the two categories is not well-defined, mainly because the rate of volatilization of a dissolved compound does not only depends on H_C, but also on the hydrodynamic properties of the phases where the transfer occurs as highlighted by the present study.

Using the results of the 2RCM, the relative liquid resistance (R_L/R_T) for each molecule as a function of P_N/V was calculated. This parameter represents the proportion of the total mass transfer resistance that is due to the liquid-phase transfer resistance. The calculation is based on Eq. (8) and the results are depicted in Figure 8. For toluene, more than 90% of the resistance correspond to the liquid side, which admits classifying it as a "volatile" compound, as expected. On the other hand, phenanthrene (less than 10% of liquid-side resistance) and naphthalene (between 20% and 40% liquid-side resistance) can be confirmed as "semi-volatile" substances at the conditions tested in this study. This means that, since three

substances tested are comprised within a wide R_L/R_T range, the conclusions of this research work may be applicable to most volatile and semi-volatile substances.

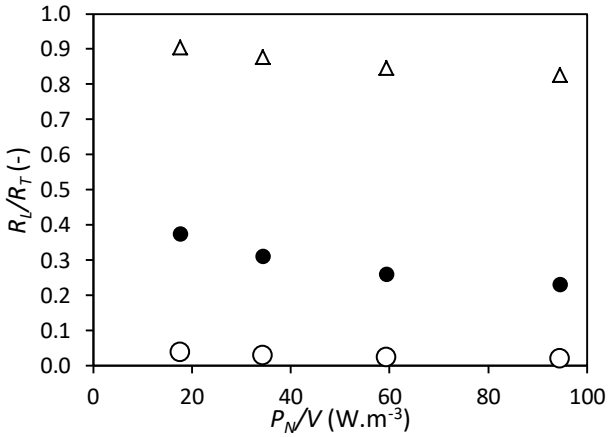

Figure 8. Relative liquid resistance for (△) Toluene, (●) Naphthalene and (○) Phenanthrene

4.5. Relevance and limitations of the models

Traditionally, in VOCs surface volatilization and stripping modeling, the gas-side resistance is considered negligible [4,6]. However, this assumption is not always correct because of the variability of the "volatile" condition of the compounds according to the process characteristics and its operating conditions as highlighted by the present study. Therefore, for semi-volatile compounds, using models that consider the gas-side resistance is a better option. Moreover, in many aerobic processes, oxygen represents a useful reference compound. Indeed, numerous oxygen mass transfer measurements methods and scale-up correlations based on oxygen exist in the literature [21]. Thus, the PCM, usually based on this molecule, is one of the most frequently used in the literature. Although the use of only one reference compound is an easy and practical way to calculate the mass transfer coefficient of other compounds, this method has several limitations. For example, only the parameters affecting exclusively the liquid phase are considered (since the gas-side resistance is negligible for this compound). In addition, several parameters should be either assumed or estimated for the specific system, i.e. the ratio of individual mass transfer coefficient and the exponents of the liquid and gas diffusivity ratio. Hsieh et al. [11] explain that the mass transfer coefficient ratio is generally assumed to be ranged between 50 and 300 (with an average of 150), which is a wide range. Besides, this parameter varies according to the hydrodynamic conditions as shown in section 4.3. In the same way, the values of m and n can significantly vary. All this may lead to wrong estimations of the mass transfer coefficient.

One may reduce the uncertainties or the estimations errors by developing an approach to calculate the gas-side resistance using the 2RCM. By directly estimating the individual mass transfer coefficients with the help of two reference compounds, this model leads to a more robust way to obtain the gas-liquid mass transfer coefficient of any compound, volatile or not. This research work has proved that, for surface volatilization, the use of water as a reference compound produces better results than the traditional PCM for semi-VOCs. The use of the 2RCM avoids the introduction of errors associated to assumptions made for the ratio of individual mass transfer coefficients. Knowing both oxygen and water transfer behaviors in the system allows accounting for liquid-film and gas-film changes, respectively. Moreover, by means of simple equipment, basic experiments on water transfer can be performed in almost any system to obtain the necessary information regarding the gas-side resistance. This implies that, if the reference compounds' gas-liquid transfer is characterized, the transfer of any volatile or semi-volatile compound can be obtained by extrapolation.

In this sense, the approach proposed in this paper can be used in wastewater treatment plants, slurry reactors, soil washing processes or any process in which HOC volatilization is non-negligible to quantify the gas-liquid mass transfer of compounds susceptible to volatilize. Nonetheless, the major limitation of this practice is that air saturation can be reached easily and rapidly, especially in systems with low or no gas-phase circulation. The same limitation applies for aerated systems using bubble diffusers within the liquid phase in which, depending on the bubble size and the physicochemical properties of the compound, few centimeters may be sufficient to reach the mass transfer equilibrium. For these cases, a similar approach, but using other substances allowing higher equilibrium concentrations in the gas phase can be used.

It is important to highlight that the extrapolation of the results of this paper for larger scales should be considered thoroughly regarding the specific conditions of the mass transfer. For instance, in large tanks open to the atmosphere, gas-side mass transfer at the surface will be largely controlled by the wind action, which will not be necessarily homogeneous along the surface of the reactor. Moreover, theoretical expressions proposed in Table 1, in which the models studied in this article are based allow an accurate representation of the mass transfer phenomena in conditions similar to the reactor condition. However, in the case of fully turbulent gas-films, modifications to the theoretical expressions should be included (e.g. eddies dynamics in the interfacial layer), which would produce complex correlations between the diffusivity and the k_Ga, hindering the application of the 2RCM [41,42].

5. Conclusions

On one hand, this study demonstrated the impact of the mechanical power input ($^{P_N}/_{V}$) on the surface volatilization. A power-type correlation was found between water, oxygen and HOC surface overall mass transfer coefficients and $^{P_N}/_{V}$. A correlation between the Henry's law constant and the exponent of the mentioned power-type correlation for the HOCs was established. These correlations can be used to estimate the extent of the impact of $^{P_N}/_{V}$ on the volatilization rate for HOCs.

On the other hand, the role of the reference compounds on the modeling of the mass transfer coefficient on volatile and semi-volatile compounds has been clarified. The 2RCM can predict the gas-liquid mass transfer coefficient with a reasonable error using only the hypothesis for fixing the diffusivity n and m. In addition, the use of the 2RCM avoids the error introduced by the estimation of the ratio of individual mass transfer coefficients if the PCM is used for semi-VOCs. This means that the former is preferable for the cases where a reference compound with gas-side controlled mass transfer can be used, due to its higher robustness and its extrapolatable characteristics regarding hydrodynamic changes in both gas-side and liquid-side interfaces.

6. Funding

This work was supported by the European Commission through the Erasmus Mundus Joint Doctorate Program "Environmental Technologies for Contaminated Solids, Soils and Sediments" ETeCoS^3 [grant agreement FPA no. 2010-0009] and the Île-de-France region through the DIM R2DS program [no. 2014-13].

7. References

[1] Y. Fayolle, A. Cockx, S. Gillot, M. Roustan, A. Héduit, Oxygen transfer prediction in aeration tanks using CFD, Chem. Eng. Sci. 62 (2007) 7163–7171. https://doi.org/10.1016/j.ces.2007.08.082.

[2] U. Hübner, U. von Gunten, M. Jekel, Evaluation of the persistence of transformation products from ozonation of trace organic compounds – A critical review, Water Res. 68 (2015) 150–170. https://doi.org/10.1016/j.watres.2014.09.051.

[3] H. Monteil, Y. Péchaud, N. Oturan, M.A. Oturan, A review on efficiency and cost effectiveness of electro- and bio-electro-Fenton processes: Application to the treatment of pharmaceutical pollutants in water, Chem. Eng. J. 376 (2019) 119577. https://doi.org/10.1016/j.cej.2018.07.179.

[4] I. Mozo, G. Lesage, J. Yin, Y. Bessiere, L. Barna, M. Sperandio, Dynamic modeling of biodegradation and volatilization of hazardous aromatic substances in aerobic bioreactor, Water Res. 46 (2012) 5327–5342. https://doi.org/10.1016/j.watres.2012.07.014.
[5] D.O. Pino-Herrera, Y. Pechaud, D. Huguenot, G. Esposito, E.D. van Hullebusch, M.A. Oturan, Removal mechanisms in aerobic slurry bioreactors for remediation of soils and sediments polluted with hydrophobic organic compounds: An overview, J. Hazard. Mater. 339 (2017) 427–449. https://doi.org/10.1016/j.jhazmat.2017.06.013.
[6] J.E. Baeten, M.C.M. van Loosdrecht, E.I.P. Volcke, When and why do gradients of the gas phase composition and pressure affect liquid-gas transfer?, Water Res. 178 (2020) 115844. https://doi.org/10.1016/j.watres.2020.115844.
[7] J. Yang, K. Wang, Q. Zhao, L. Huang, C.-S. Yuan, W.-H. Chen, W.-B. Yang, Underestimated public health risks caused by overestimated VOC removal in wastewater treatment processes, Env. Sci Process. Impacts. 16 (2014) 271–279. https://doi.org/10.1039/C3EM00487B.
[8] Y. Luo, W. Guo, H.H. Ngo, L.D. Nghiem, F.I. Hai, J. Zhang, S. Liang, X.C. Wang, A review on the occurrence of micropollutants in the aquatic environment and their fate and removal during wastewater treatment, Sci. Total Environ. 473–474 (2014) 619–641. https://doi.org/10.1016/j.scitotenv.2013.12.065.
[9] M. Pomiès, J.-M. Choubert, C. Wisniewski, M. Coquery, Modelling of micropollutant removal in biological wastewater treatments: A review, Sci. Total Environ. 443 (2013) 733–748. https://doi.org/10.1016/j.scitotenv.2012.11.037.
[10] J.R. Mihelcic, C.R. Baillod, J.C. Crittenden, T.N. Rogers, Estimation of VOC Emissions from Wastewater Facilities by Volatilization and Stripping, Air Waste. 43 (1993) 97–105. https://doi.org/10.1080/1073161X.1993.10467120.
[11] C. Hsieh, K.S. Ro, M.K. Stenstrom, Estimating emissions of 20 VOCs. I: Surface aeration, J. Environ. Eng. 119 (1993) 1077–1098.
[12] A.V. Padalkar, R. Kumar, Removal mechanisms of volatile organic compounds (VOCs) from effluent of common effluent treatment plant (CETP), Chemosphere. 199 (2018) 569–584. https://doi.org/10.1016/j.chemosphere.2018.01.059.
[13] C. Munz, P.V. Roberts, Gas- and liquid-phase mass transfer resistances of organic compounds during mechanical surface aeration, Water Res. 23 (1989) 589–601. https://doi.org/10.1016/0043-1354(89)90026-2.
[14] J.H. Smith, D.C. Bomberger, D.L. Haynes, Volatilization rates of intermediate and low volatility chemicals from water, Chemosphere. 10 (1981) 281–289.
[15] C. Hsieh, R.W. Babcock, M.K. Stenstrom, Estimating Emissions of 20 VOCs. II: Diffused Aeration, J. Environ. Eng. 119 (1993) 1099–1118. https://doi.org/10.1061/(ASCE)0733-9372(1993)119:6(1099).
[16] R. Sander, Compilation of Henry's law constants (version 4.0) for water as solvent, Atmospheric Chem. Phys. 15 (2015) 4399–4981. https://doi.org/10.5194/acp-15-4399-2015.
[17] D. Mackay, W.Y. Shiu, R.P. Sutherland, Determination of air-water Henry's law constants for hydrophobic pollutants, Environ. Sci. Technol. 13 (1979) 333–337. https://doi.org/10.1021/es60151a012.
[18] J.-C. Charpentier, Mass-Transfer Rates in Gas-Liquid Absorbers and Reactors, in: T.B. Drew, G.R. Cokelet, J.W. Hoopes, T. Vermeulen (Eds.), Adv. Chem. Eng., Academic Press, 1981: pp. 1–133. https://doi.org/10.1016/S0065-2377(08)60025-3.
[19] A. Cockx, Z. Do-Quang, J.M. Audic, A. Liné, M. Roustan, Global and local mass transfer coefficients in waste water treatment process by computational fluid dynamics, Chem. Eng. Process. Process Intensif. 40 (2001) 187–194. https://doi.org/10.1016/S0255-2701(00)00138-0.

[20] M.N. Kashid, A. Renken, L. Kiwi-Minsker, Gas–liquid and liquid–liquid mass transfer in microstructured reactors, Chem. Eng. Sci. 66 (2011) 3876–3897. https://doi.org/10.1016/j.ces.2011.05.015.
[21] F. Garcia-Ochoa, E. Gomez, Bioreactor scale-up and oxygen transfer rate in microbial processes: An overview, Biotechnol. Adv. 27 (2009) 153–176. https://doi.org/10.1016/j.biotechadv.2008.10.006.
[22] W.K. Lewis, W.G. Whitman, Principles of Gas Absorption., Ind. Eng. Chem. 16 (1924) 1215–1220. https://doi.org/10.1021/ie50180a002.
[23] R. Higbie, Penetration theory leads to use of the contact time in the calculation of the mass transfer coefficients in the two film theory, Trans Am Inst Chem Engrs 31. 365 (1935).
[24] P.V. Danckwerts, Significance of Liquid-Film Coefficients in Gas Absorption, Ind. Eng. Chem. 43 (1951) 1460–1467. https://doi.org/10.1021/ie50498a055.
[25] J. Arogo, R.H. Zhang, G.L. Riskowski, L.L. Christianson, D.L. Day, Mass Transfer Coefficient of Ammonia in Liquid Swine Manure and Aqueous Solutions, J. Agric. Eng. Res. 73 (1999) 77–86. https://doi.org/10.1006/jaer.1998.0390.
[26] S. Soltanali, Z. Shams Hagani, Modeling of air stripping from volatile organic compounds in biological treatment processes, Int. J. Environ. Sci. Technol. 5 (2008) 353–360. https://doi.org/10.1007/BF03326030.
[27] F. Heymes, L. Aprin, A. Bony, S. Forestier, S. Cirocchi, G. Dusserre, An experimental investigation of evaporation rates for different volatile organic compounds, Process Saf. Prog. 32 (2013) 193–198. https://doi.org/10.1002/prs.11566.
[28] T. Poós, E. Varju, Mass transfer coefficient for water evaporation by theoretical and empirical correlations, Int. J. Heat Mass Transf. 153 (2020) 119500. https://doi.org/10.1016/j.ijheatmasstransfer.2020.119500.
[29] D.O. Pino-Herrera, Y. Fayolle, S. Pageot, D. Huguenot, G. Esposito, E.D. van Hullebusch, Y. Pechaud, Gas-liquid oxygen transfer in aerated and agitated slurry systems with high solid volume fractions, Chem. Eng. J. 350 (2018) 1073–1083. https://doi.org/10.1016/j.cej.2018.05.193.
[30] S. Hall, Rules of Thumb for Chemical Engineers, Elsevier Science, 2017.
[31] C. Munz, P.V. Roberts, Air-Water Phase Equilibria of Volatile Organic Solutes, J. Am. Water Works Assoc. 79 (1987) 62–69.
[32] P.R. Lowe, An approximating polynomial for the computation of saturation vapor pressure, J. Appl. Meteorol. 16 (1977) 100–103.
[33] C.V. Chrysikopoulos, L.M. Hildemann, P.V. Roberts, Modeling the emission and dispersion of volatile organics from surface aeration wastewater treatment facilities, Water Res. 26 (1992) 1045–1052.
[34] J.A. Libra, Volatilization of organic compounds in an aerated stirred tank reactor, University of California, Los Angeles, 1991. http://www.seas.ucla.edu/stenstro/d/d11.pdf (accessed December 11, 2016).
[35] H.D. Monteith, J.P. Bell, W.J. Parker, H. Melcer, R.T. Harvey, Effect of Bubble-Induced Surface Turbulence on Gas-Liquid Mass Transfer in Diffused Aeration Systems, Water Environ. Res. 77 (2005) 128–137.
[36] C. Matter-Müller, W. Gujer, W. Giger, Transfer of volatile substances from water to the atmosphere, Water Res. 15 (1981) 1271–1279.
[37] P.V. Roberts, C. Munz, P. Dändliker, Modeling Volatile Organic Solute Removal by Surface and Bubble Aeration, J. Water Pollut. Control Fed. 56 (1984) 157-.
[38] L. Lucattini, G. Poma, A. Covaci, J. de Boer, M.H. Lamoree, P.E.G. Leonards, A review of semi-volatile organic compounds (SVOCs) in the indoor environment: occurrence in

consumer products, indoor air and dust, Chemosphere. 201 (2018) 466–482. https://doi.org/10.1016/j.chemosphere.2018.02.161.
[39] K.T. Valsaraj, R. Ravikrishna, J.J. Orlins, J.S. Smith, J.S. Gulliver, D.D. Reible, L.J. Thibodeaux, Sediment-to-air mass transfer of semi-volatile contaminants due to sediment resusmension in water, Adv. Environ. Res. (1997) 13.
[40] V. Martí, J. De Pablo, I. Jubany, M. Rovira, E. Orejudo, Water-Air Volatilization Factors to Determine Volatile Organic Compound (VOC) Reference Levels in Water, Toxics. 2 (2014) 276–290. https://doi.org/10.3390/toxics2020276.
[41] W. Brutsaert, A theory for local evaporation (or heat transfer) from rough and smooth surfaces at ground level, Water Resour. Res. 11 (1975) 543–550. https://doi.org/10.1029/WR011i004p00543.
[42] A.A. Prata, J.M. Santos, V. Timchenko, R.M. Stuetz, A critical review on liquid-gas mass transfer models for estimating gaseous emissions from passive liquid surfaces in wastewater treatment plants, Water Res. 130 (2018) 388–406. https://doi.org/10.1016/j.watres.2017.12.001.

Appendix A. Theoretical considerations for Henry's law constant determination

The mass transfer rate by bubble volatilization is given by Eq. (A.1.) In this case, the transfer area is the interface between the dispersed bubbles in the liquid phase and the liquid phase itself (A_B).

$$V_G \frac{dC_G}{dt} = K_L A^B \left(C_L^{*,B} - C_L\right) \tag{A.1}$$

Where V_G the total gas phase volume in the bubbles and the superscript is B refers to bubbles. Under certain conditions, it is possible to assume that the variation of C_L is negligible in relation to the variation of C_G inside a single bubble rising through the reactor. Therefore, C_L can be considered constant for the integration of Eq. (A.1). Then, using Eq. (3) and integrating in time from the moment in which a bubble enters into the reactor ($C_G = 0$) to the moment it exits ($C_G = C_G^{out}$) (i.e. the gas residence time) and for all the bubbles dispersed in the gas phase, Eq. (A.2) is obtained.

$$ln\left|1 - \frac{C_G^{out}}{Hc.C_L}\right| = -\frac{K_L a^B V_L}{H_C V_G} t_r \tag{A.2}$$

Where t_r is the residence time of the gas in the reactor and is defined as $t_r = \frac{V_G}{Q_G}$. If Eq. (A.2) is rearranged by using the relations established in Eq. (A.3) derived from Henry's law (which defines the saturation degree), it is possible to obtain the concentration of the desired compound in the bubble when it reaches the surface of the liquid as a function of the mass transfer coefficient, the Henry's law constant and the operational parameters of the reactor V_L and Q_G (Eq. (A.4)).

$$\frac{C_G^{out}}{C_G^{*,B}} = S_d \tag{A.3}$$

$$S_d = 1 - e^{\frac{K_L a^B V_L}{H_C Q_G}} \tag{A.4}$$

According to Matter-Müller et al. [36], a mass balance in the liquid phase of a reactor in which only bubble volatilization occurs would lead to Eq. (A.5). Invoking Henry's law (Eq. (3)) and using Eq. (A.3) it is possible to obtain Eq. (A.6).

$$V_L \frac{dC_L}{dt} = -Q_G C_G^{out} \tag{A.5}$$

$$C_G^{out} = S_d H_C C_L \tag{A.6}$$

747

748 By combining and rearranging Eq. (A.5) and Eq. (A.6), it is possible to obtain Eq. (A.7).
749 Then, if the concentration of the volatile compound in the liquid phase is recorded in time, a
750 first order curve may be plotted, from which it can be possible to calculate the saturation
751 degree and, hence, the diffused mass transfer coefficient. A linear correlation may be found
752 between the natural logarithm of the normalized concentration of the volatilized product and
753 time, and the slope of this correlation, Sp^B, can be defined by Eq. (A.8).

$$\frac{dC_L}{dt} = -\left(\frac{Q_G H_C}{V_L} S_d\right) C_L \tag{A.7}$$

$$Sp^B = -\frac{Q_G H_C}{V_L} S_d \tag{A.8}$$

754

755 Hsieh et al. [36] consider three cases regarding the saturation degree in the bubble: i) when
756 $S_d \leq 0.1$, the slope, Sp^B is approximately equal to the bubble mass transfer coefficient; ii)
757 when $S_d \geq 0.99$, the bubbles exit the liquid phase near saturation and the slope will
758 approximate $-\frac{Q_G H_C}{V_L}$ and iii) when $0.1 \geq S_d \geq 0.99$, the mass transfer coefficient can be
759 calculated using the expressions in Eq. (A.4) and Eq. (A.8). When bubble saturation (case ii)
760 is reached in a range of air flows, a linear correlation between Sp^B and Q_G can be obtained
761 and, using the slope of this correlation, it is possible to calculate accurately the Henry's law
762 constant of a particular compound using Eq. (A.8) and assuming S_d = 1 [17].

763

764

765

766

767

768

769

770

771

772

773

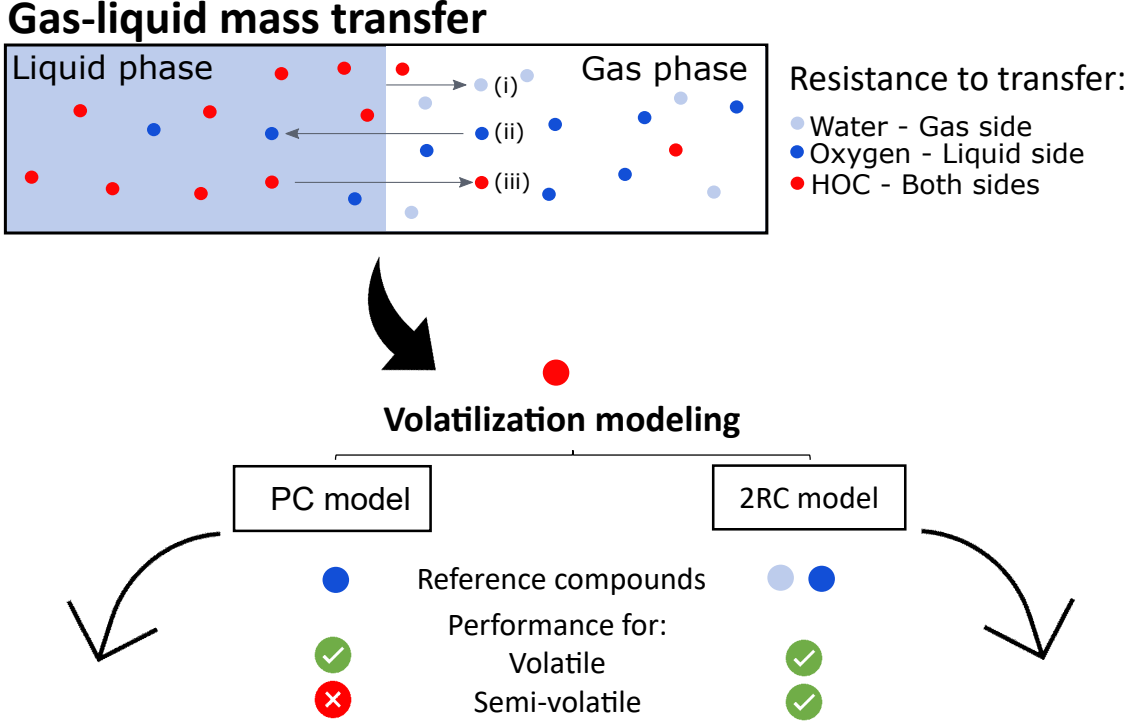

$$\Psi = \frac{K_L a^S_{HOC}}{K_L a^S_{O_2}} = \frac{1}{\frac{1}{\left(\frac{D_{L,HOC}}{D_{L,O_2}}\right)^n} + \frac{1}{H_C\left(k_G a^S_{O_2}/k_L a^S_{O_2}\right)\left(\frac{D_{G,HOC}}{D_{G,O_2}}\right)^m}}$$

$$\frac{1}{K_L a^S_{HOC}} = \frac{1}{k_L a^S_{O_2}\left(\frac{D_{L,HOC}}{D_{L,O_2}}\right)^n} + \frac{1}{H_C k_G a^S_W \left(\frac{D_{G,HOC}}{D_{G,W}}\right)^m}$$